Supporting Information

Electrochemical Degradation Mechanisms of Commercial Carbon-Supported Gold Nanoparticles in Acidic Media

Milutin Smiljanić[a,b], Urša Petek[a], Marjan Bele[a], Francisco Ruiz-Zepeda[a,c], Martin Šala[d], Primož Jovanovič[a], Miran Gaberščček[a,e], Nejc Hodnik[a,f]

[a]*Department of Materials Chemistry, National Institute of Chemistry*

Hajdrihova 19, 1000 Ljubljana, Slovenia

[b]*Laboratory for Atomic Physics, Institute for Nuclear Sciences Vinča, University of Belgrade, Mike Alasa 12-14, 11001 Belgrade, Serbia*

[c]*Department of Physics and Chemistry of Materials, Institute of Metals and Technology, Lepi pot 11, 1000 Ljubljana, Slovenia*

[d]*Department of Analytical Chemistry, National Institute of Chemistry*

Hajdrihova 19, 1000 Ljubljana, Slovenia

[e]*Faculty of Chemistry and Chemical Technology University of Ljubljana, Večna pot 113, 1000 Ljubljana*

[f]*University of Nova Gorica, Vipavska 13, 5000 Nova Gorica, Slovenia*

milutin.smiljanic@ki.si, *nejc.hodnik@ki.si*

TEM characterization of Au/C sample.

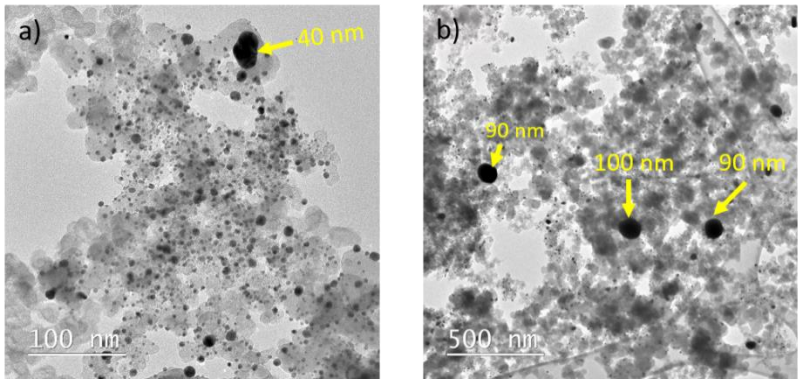

Figure S1. TEM imaging of the pristine Au/C sample showing polydispersity of the sample in the terms of particle size distribution. Yellow arrows highlight a few particularly large particles. Such particles were seldom observed on the Au/C sample and due to their low number they were not included in particle size distribution.

Electrochemical activation of Au/C films in RDE setup.

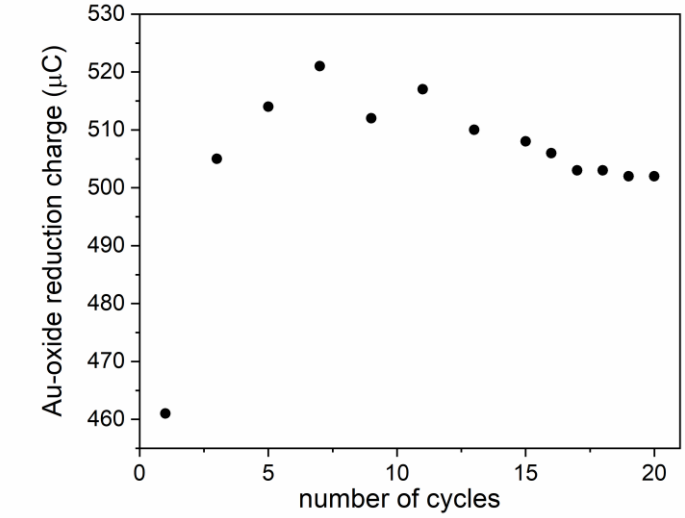

Figure S2. Development of Au ESA during activation of Au/C films in RDE setup by 20 voltammetric scans at 100 mV/s in the potential window between -0.02 V_{RHE} and 1.63 V_{RHE}. Charge corresponding to Au-oxide reduction for every second voltammogram is presented up to the 15th cycle, followed by the addition of the last five points (16th to 20th cycle) to emphasize stabilization of Au ESA at the end of activation procedure.

Monitoring of the changes in gold electrochemical surface area during AST.

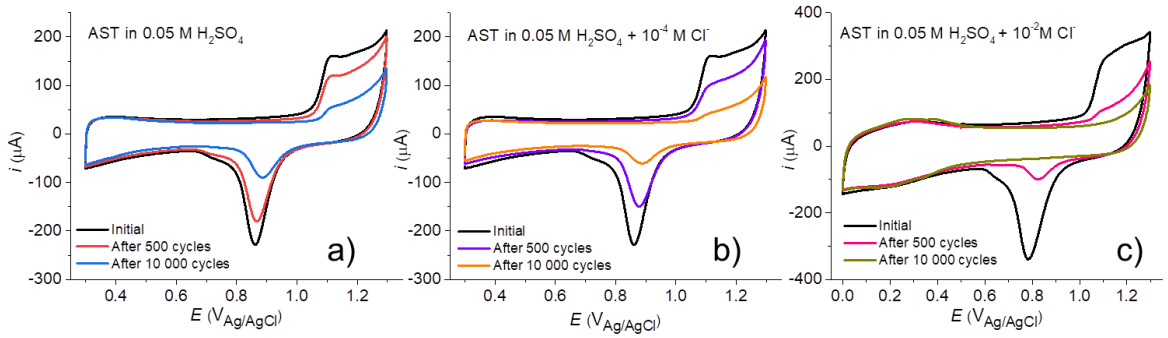

Figure S3. Cyclic voltammograms sequentially recorded during AST in: (a) 0.05 M H_2SO_4 (50 mV/s); (b) 0.05 M H_2SO_4 + 10^{-4} M Cl^- (50 mV/s) and (c) 0.05 M H_2SO_4 + 10^{-2} M Cl^- (100 mV/s). CVs presented in Figs. S3a and S3b were recorded in the same electrolytes in which ASTs were performed. Due to the strong influence of the increased amount of chlorides (10^{-2} M) on gold oxidation/reduction processes, CVs presented in Fig. S4 were recorded in a separate electrochemical cell containing neat 0.05 M H_2SO_4 electrolyte and different counter electrode and reference Ag/AgCl electrode. Different potential range and scan rate in Fig. S4c than in Figs. S3a and S3b were used unintentionally. All potential scales are given versus used Ag/AgCl reference electrodes.

Influence of different UPLs during AST on the loss of Au ESA. Comparison of the influence of potentiostatic and potentiodynamic conditions at the same UPL on the loss of Au ESA.

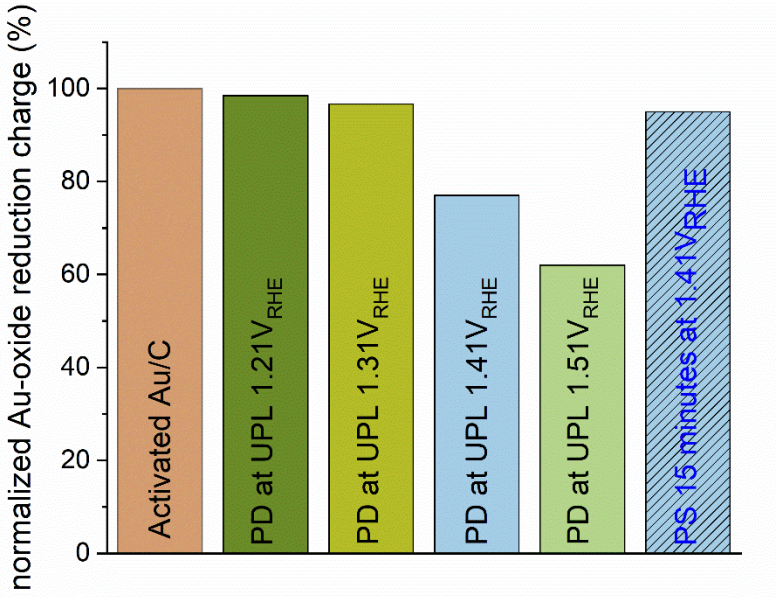

Figure S4. Influence of different potentiodynamic (PD) and potentiostatic (PS) treatments on the loss of gold electrochemical surface area of Au/C samples. Activated Au/C refers to the values for Au-oxide reduction charge obtained at the end of electrochemical activation. PD treatments consisted of 500 fast scans (1 V/s) in the potential range between –0.02 V_{RHE} and different UPLs indicated in the graph. PS treatment was performed by holding the electrode potential at1.41 V_{RHE} over 15 minutes, which is the time comparable for the 500 fast scans (1 V/s) at the same UPL. For the sake of comparison of Au ESA, set of two cyclic voltammograms was recorded under the same conditions as in activation at the end of each PD or PS experiment.

Effect of AST degradation on the dissolution profile of the Au/C as determined by EFC-ICP-MS.

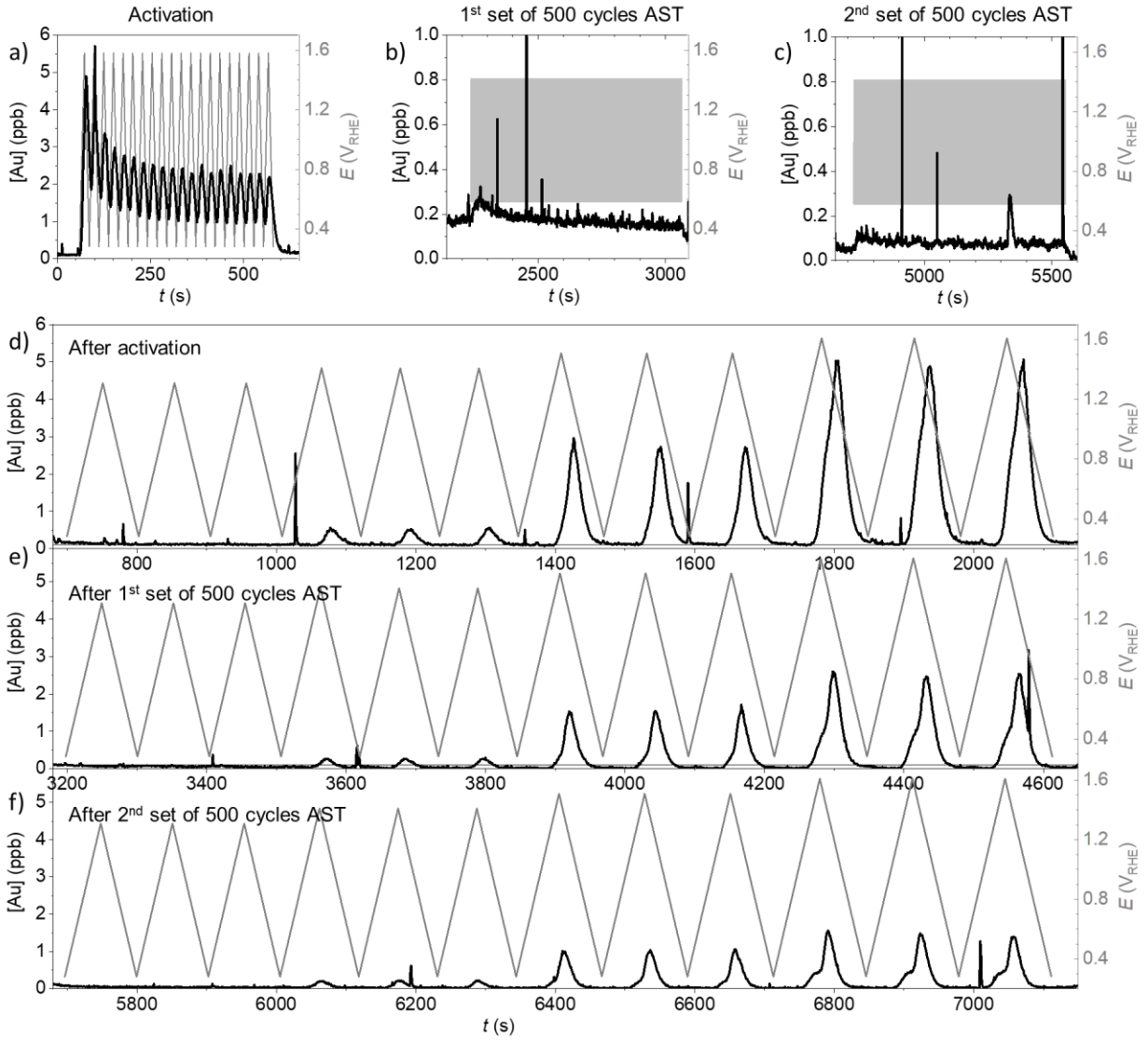

Figure S5. EFC-ICP-MS dissolution profiles of Au as a function of the applied potential cycles. For an overview of the experiment, see Figure 4a. (a) The activation protocol (20 cycles at 100 mV/s from 0.28 to 1.58 V_{RHE}); (b) 500 AST cycles of degradation at 1 V/s between 0.58 and 1.41 V_{RHE}; (c) another 500 degradation cycles under the same conditions. Each of these protocols was followed by dissolution profiling, shown on (d) before degradation; (e) after 500 cycles of AST degradation and (f) after additional 500 cycles of AST (1000 in total). In each case, three

potential cycles with 20 mV/s scan rate were repeated from 0.28 V_{RHE} to an UPL before increasing it by 0.10 V (UPLs: 1.31; 1.41; 1.51 and 1.61 V_{RHE}). The axis to the right shows Au concentration and the axis on the left electrode potential.

Changes of the amounts of anodically and cathodically dissolved Au caused by AST.

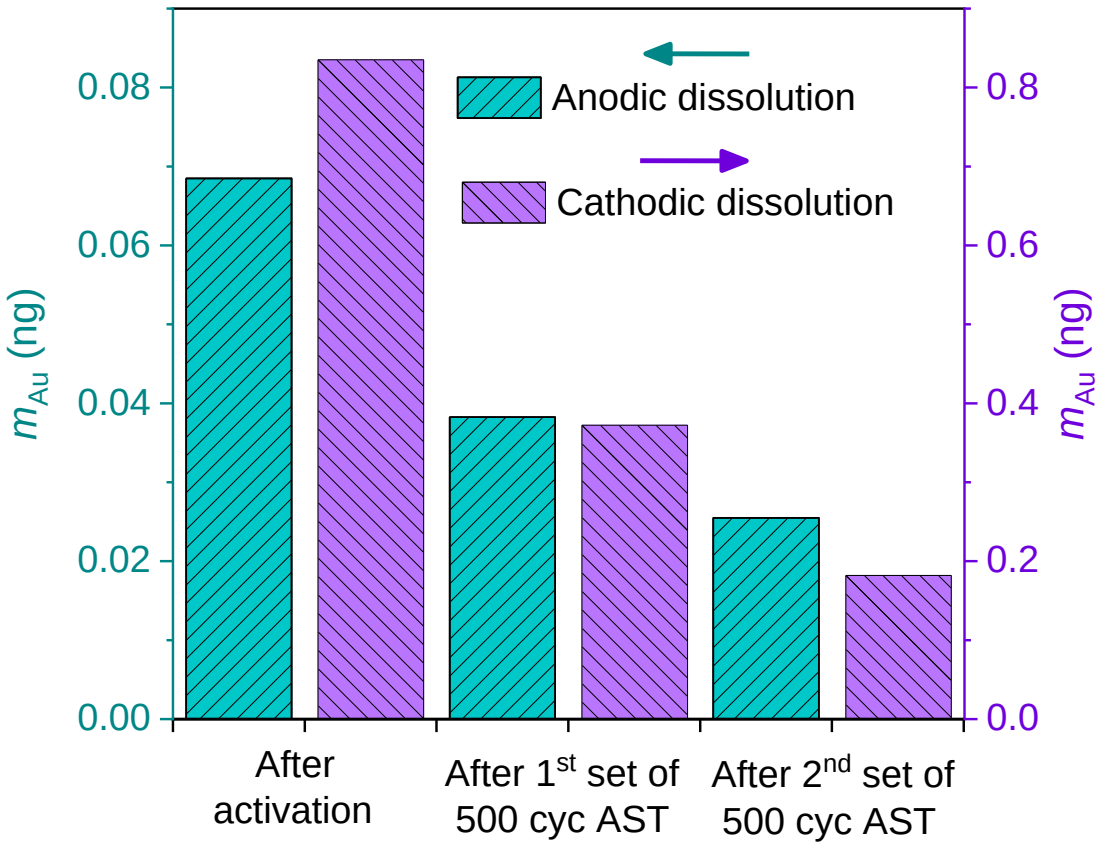

Figure S6. Integrals of Au dissolution peaks recorded in EFC-ICP-MS during the potential profiling protocol from Figure S5 and Figure 4. The peaks with the UPL of 1.61 V_{RHE} were deconvoluted into an anodic contribution (peak coincides with E(t) peak) and a transient cathodic contribution.

Particle size distribution with distributions of mass and surface area.

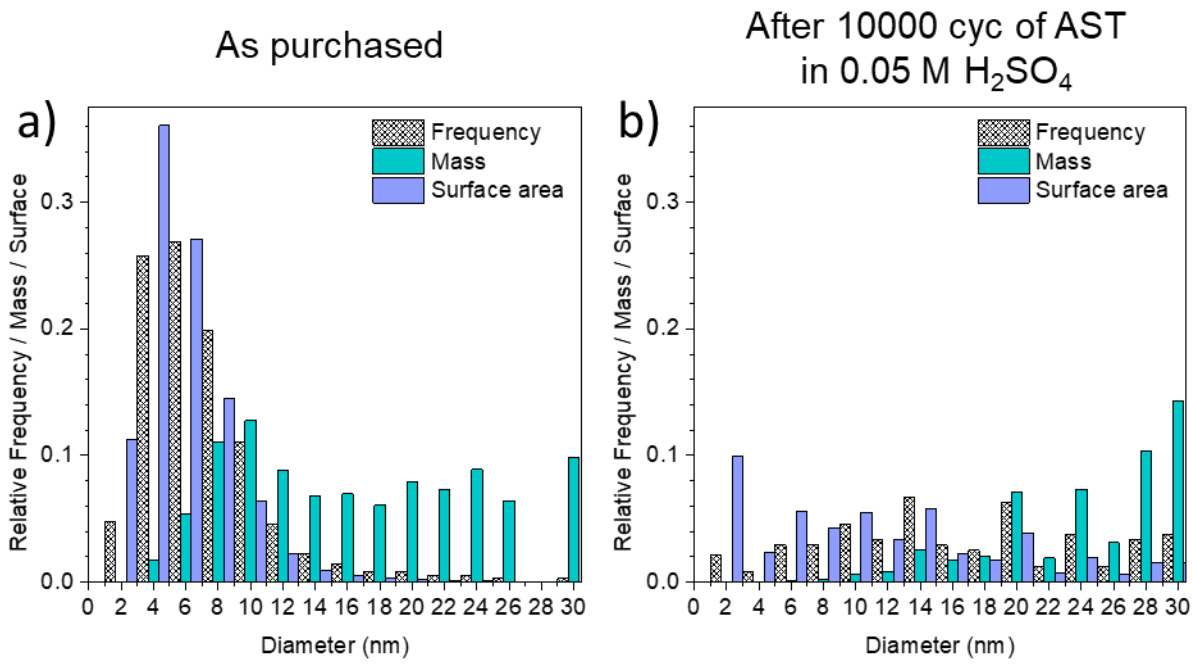

Figure S7. Particle size distribution (PSD) based on STEM image analysis (a) for the as-purchased Au/material and (b) after 10 000 cycles of degradation in 0.05 M H_2SO_4. The mass and surface fractions were calculated for a population of ideally spherical particles with the given frequency distribution. It is important to note that only particles with diameters smaller than 30 nm were taken into account for PSD and the larger particles – although observed under TEM – were intentionally excluded.

Electrochemistry – mass spectrometry (EC-MS) for monitoring carbon corrosion through evolution of CO_2.

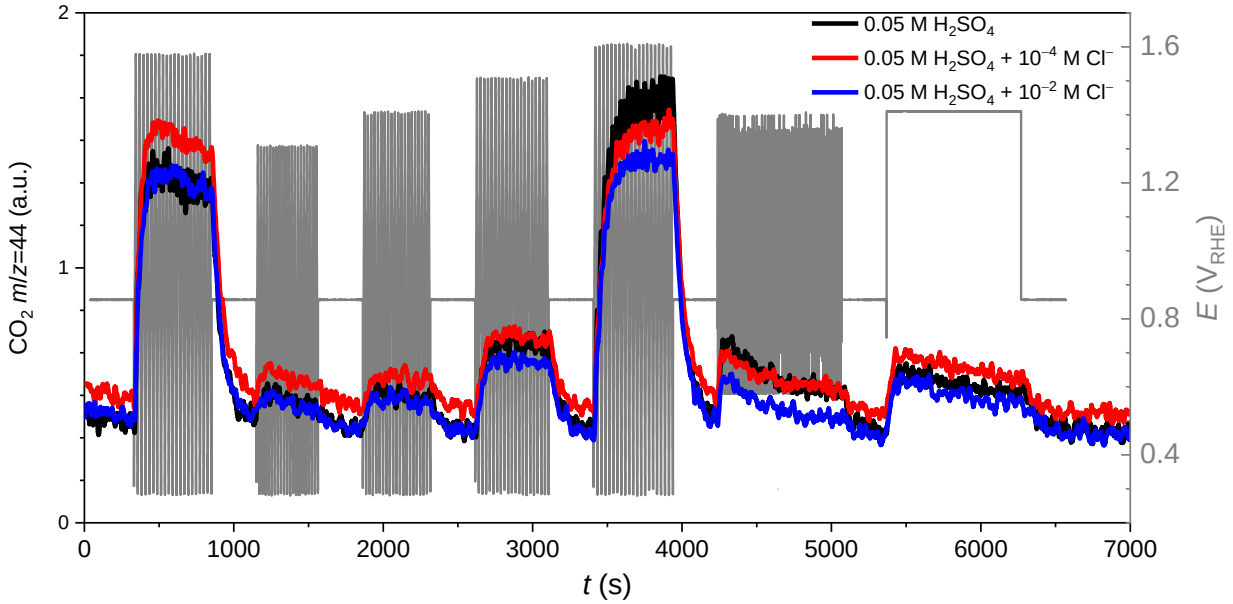

Figure S8. EC-MS dissolution profiles showing the signal for m/z = 44, attributed to CO_2, as a function of electrode potential. The experiment was performed in 0.05 M H_2SO_4 (as on Figure 5) and additionally in 0.05 M H_2SO_4 + 10^{-4} M Cl^- and in 0.05 M H_2SO_4 + 10^{-2} M Cl^-. The electrochemical protocol consisted of 20 activation cycles (100 mV/s, 0.28–1.58 V_{RHE}), followed by sets of 20 cycles (100 mV/s) from 0.28 V_{RHE} to increasing UPL, namely 1.31, 1.41, 1.51 and 1.61 V_{RHE}. This was followed by AST (500 cycles, 1 V/s, 0.58–1.41 V_{RHE} and a 15 min potential hold at 1.41 V_{RHE}. Sets of cycles were separated by 5 min of open circuit potential to allow for background stabilization.